A Novel Fusion Algorithm for Visible and Infrared Image using Non-subsampled Contourlet Transform and Pulse-coupled Neural Network

Chihiro Ikuta[1], Songjun Zhang[2], Yoko Uwate[1], Guoan Yang[3] and Yoshifumi Nishio[1]
[1]*Department of Electrical and Electronic Engineering, Tokushima University, 2-1 Minami-Josanjima, Tokushima, Japan*
[2]*Department of Computing Mathematics School of Science, Xi'an Jiaotong University, No.28 Xianning West Road, Xi'an City, Shaanxi Province, China*
[3]*Department of Automation Science and Technology, School of Electronic and Information Engineering, Xi'an Jiaotong University, No.28 Xianning West Road, Xi'an City, Shaanxi Province, China*
{*ikuta, uwate, nishio*}*@ee.tokushima-u.ac.jp, youyi000@gmail.com, gayang@mail.xjtu.edu.cn*

Keywords: Image Fusion, Visible Image, Infrared Image, Pulse Coupled Neural Network, Non-subsampled Contourlet Transform.

Abstract: An image fusion algorithm between visible and infrared images is significant task for computer vision applications such as multi-sensor systems. Among them, although a visible image is clear perfectly able to be seen through the naked eyes, it is often suffers with noise; while an infrared image is unclear but it has high anti-noise property. In this paper, we propose a novel image fusion algorithm for visible and infrared images using a non-subsampled contourlet transform (NSCT) and a pulse-coupled neural network (PCNN). First, we decompose two original images above mentioned into low and high frequency coefficients based on the NSCT. Moreover, each low frequency coefficients for both images are duplicated at multiple scales, and are processed by laplacian filter and average filter respectively. Finally, we can fuse the normalized coefficients by using the PCNN. Conversely, we can reconstruct a fused image based on the low and high frequency coefficients, which are fused by using the inverse NSCT. Experimental results show that the proposed image fusion algorithm surpasses the conventional and state-of-art image fusion algorithm.

1 INTRODUCTION

Image fusion plays an important role in the computer vision and image processing fields. In recent years, many image fusion algorithm are applied to computer vision, pattern recognition and image processing fields such as multi-focus and multi-sensors image fusion, and so on (Xu and Chen, 2004) (Wang et al., 2008) (Qu et al., 2008). Especially, an image fusion algorithm between visible and infrared images is significant for computer vision and image processing applications. The contourlet transform is a new two-dimensional extension of the wavelet transform using multi-scale and directional filter banks (Yang et al., 2010). And then, a non-subsampled contourlet transform (NSCT) is developed by Da Cunha, Zhou and Do (da Cunha et al., 2006). The NSCT has a fully shift invariant property than the contourlet, leads to better frequency selectivity, directivity and regularity (Zhou et al., 2005). On the other hand, we know that a pulse-coupled neural network (PCNN) is presented by Eckhorn in 1990 (Eckhorn, 1990). This method is developed based on the experimental observations of synchronous pulse bursts in cat cortex. It is characterized by the global coupling and pulse synchronization of neurons. And the PCNN has excellent performance in image edge detection applications. Recently, several image fusion algorithm based on the NSCT and PCNN have been developed, for example, based on spatial frequency-motivated PCNN in NSCT domain of Qu (Qu et al., 2008), stationary wavelet-based NSCT and PCNN of Yang (Yang et al., 2009), based on NSCT-PCNN of Ge for visible and infrared image (Ge and Li, 2010), a simplified PCNN in NSCT domain of Liu (Liu et al., 2012), and so on. These image fusion algorithm implemented better fusion performance for various image processing applications.

However, hardly any work based on NSCT-PCNN algorithm for the visible and infrared image. Therefore, in this paper, we consider to utilize the NSCT for implementing multi-scale decomposition, and PCNN

for implementing image fusion. Furthermore, we propose a novel images fusion algorithm for visible and infrared image based on the NSCT and PCNN. And the quality of a fusion image is improved by using the PCNN for the low frequency coefficients in NSCT domain. In order to the purpose, we employed two different filters, which are average filter and laplacian filter before image fusion using the PCNN, and better image fusion performance is demonstrated than based on the PCNN only.

This paper is organized as follows. In section 2, we describe an image fusion algorithm used the NSCT and PCNN. In section 3, we propose the new image fusion algorithm for visible and infrared images. In section 4, we show the experimental results, and compare with the conventional method about image fusion. Finally, in section 5, we state the conclusion and future works.

2 IMAGE FUSION ALGORITHM

Generally, the image fusion algorithm above mentioned mainly has three steps. In the first step, images are decomposed into some coefficients by the NSCT decomposition algorithm. In the next step, the coefficients from two images are compared and fused by the PCNN. Finally, the fused coefficients reconstruct into one new image by the NSCT reconstruction algorithm.

2.1 NSCT

The NSCT is compatible with the image fusion by using the PCNN, because this method does not exist the up sampling and down sampling (Zhou et al., 2005). The NSCT use pyramid filter banks to implement a multi-scale decomposition and a directional decomposition as shown in Fig. 1 (da Cunha et al., 2006). In the case of multi-scale decomposition, an image is decomposed into the low frequency coefficients and high frequency coefficients, and these operations are repeated at different scale. After that, the coefficients is decomposed into directional components in the high frequency banks.

2.2 PCNN

Eckhorn proposed a neural network model from cat's visual cortex in 1990 (Eckhorn, 1990). The PCNN is proposed by Thomas for the application of this mechanism in 1998 (Lindblad and Kinser, 2005). It is known that this method can be applied to the image processing, in addition can also be applied to image

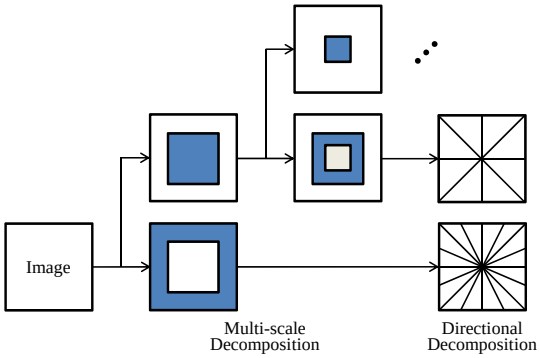

Figure 1: The non-subsampled contourlet transform for the image decomposition.

fusion (Jhonson and Padgett, 1999). When we apply the PCNN to an image processing, one pixel data in an image inputs the one neuron. Accepters of neuron are composed of a feeding part and a linking part, as follows. The feeding part is described by Eq. (1).

$$F_{ij}^{lk}(n) = S_{ij}^{lk}, \tag{1}$$

where F is an output of feeding part and S is an external stimulus. Eq. (2) is the linking part.

$$\begin{aligned} L_{ij}^{lk}(n) &= e^{-\alpha_L} L_{ij}^{lk}(n-1) \\ &\quad + V_L \textstyle\sum_{pq} W_{ij,pq}^{lk} Y_{ij,pq}^{lk}(n-1), \end{aligned} \tag{2}$$

where L is an output of linking part, V is a normalization coefficient and W is a weight to connect other neurons. An internal state is calculated by outputs of the feeding and linking part as shown in Eq. (3).

$$U_{ij}^{lk}(n) = F_{ij}^{lk}(n)\{1+\beta L_{ij}^{lk}(n)\}, \tag{3}$$

where U is an internal state. The output of neuron is calculated from comparison between the internal state and a threshold. The threshold is described by Eq. (4).

$$\theta_{ij}^{lk}(n) = e^{-\alpha_\theta}\theta_{ij}^{lk}(n-1) + V_\theta Y_{ij}^{lk}(n-1), \tag{4}$$

where θ is a threshold. In the PCNN, an activation function is a step function. The output of the neuron is described by Eq. (5).

$$Y_{ij}^{lk} = \begin{cases} 1, & U_{ij}^{lk}(n) > \theta_{ij}^{lk}(n) \\ 0, & otherwise. \end{cases} \tag{5}$$

We choose these parameters by heuristic. In this condition, we tune that the conventional method has become more high performance, and the model of PCNN shown in Fig. 2.

In the simulation, the PCNN is inputted in the decomposition coefficients of two images. In the application for the image processing, the one neuron receive one pixel of the coefficients. Thus, the number of neurons depend on the image size. The PCNN iterates process to the number of times. After that,

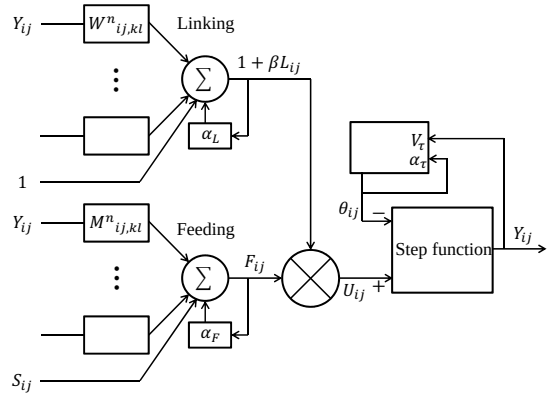

Figure 2: Block diagram of a single neuron of the PCNN.

the two images which are processed by the PCNN are compared and are fused by Eq. (6).

$$I_{ij}^{lk} = \begin{cases} A_{ij}^{lk}, & Y_{ij,A}^{lk} > Y_{ij,B}^{lk} \\ B_{ij}^{lk}, & otherwise, \end{cases} \tag{6}$$

where I is an fused image, A is coefficients of the image A, and B is coefficients of the image B.

3 PROPOSED IMAGE FUSION ALGORITHM

In this paper, we introduce a novel image fusion processing for the low frequency coefficients. Generally, the high frequency region of an image include the edge and texture information, the low frequency region concentrate almost of power for an image. Whereas image energy of the most natural scenes is mainly concentrated in the low frequency region. Hence, we consider that the quality of an image can be improved by tuning the low frequency of image.

Process of proposed image fusion algorithm is illustrated in Fig. 3. Firstly, we decompose two image into the low frequency coefficients and the high frequency coefficients by the NSCT. In addition, each low frequency coefficients for both images are duplicated at multiple scales. And then, on one hand, the coefficients is filtering by the laplacian filter expressed in Eq. (7). The laplacian filter is an edge detection operator, it can enhance the edge effects of an image. On the other hand, the coefficient is filtered by the average filter shown in Eq. (8). The average filter simplified the all of low coefficients, and can fuse the both coefficients which is normalized from the laplacian and average filter for increasing the intensity of an image in the low frequency domain.

$$Laplacian filter = \begin{bmatrix} -1 & -1 & -1 \\ -1 & 9 & -1 \\ -1 & -1 & -1 \end{bmatrix} \tag{7}$$

$$Average filter = \begin{bmatrix} 0.11 & 0.11 & 0.11 \\ 0.11 & 0.12 & 0.11 \\ 0.11 & 0.11 & 0.11 \end{bmatrix} \tag{8}$$

After filter process, we normalize the two coefficients. The two coefficients are fused by the PCNN image fusion algorithm. We process coefficients of image A and image B, and the two fused coefficients are fused by using Eq. (6). As shown in Fig. 3, the images are decomposed five levels by the pyramidal filter bank of NSCT. Thereby, the coefficient of five different frequency bands are generated, respectively. Among them, we mainly used filtering technique for the low frequency bands, which are two lower frequency levels. There realized the fusion processing for visible image and infrared image using the algorithm above. Finally, the both fused coefficient above mentioned from two different images are fused by the PCNN, and the high frequency coefficients are further decomposed to be directional band coefficient which fused by the PCNN, it is called as the second fusion for visible image and infrared image separately. Therefore, we can reconstruct the visible and infrared image using all the low and high frequency coefficient by the inverse NSCT. We investigated that the quality of a fused image is improved by filtering the low frequency coefficients. It is because that laplacian filter and average filter increased an intensity of image in the low frequency.

4 SIMULATIONS

In this section, we show the computer simulation of proposed image fusion algorithm. Here use two kinds of image sets, and investigate the image fusion performance. Furthermore, we analyze the quality of image fusion for the proposed algorithm with the low frequency coefficients to the PCNN and high frequency coefficients to the PCNN. And that parameters of the PCNN are set as $p \times q = 3 \times 3$, $\alpha_L = 1.0$, $\alpha_\theta = 0.2$, $\beta = 3$, $V_L = 1.0$, $V_\theta = 20$,

$$W = \begin{bmatrix} 0.707 & 1 & 0.707 \\ 1 & 0 & 1 \\ 0.707 & 1 & 0.707 \end{bmatrix},$$

and the maximal iteration number is $n = 200$. Here, we adopted three kinds of methods exist for evaluating image fusion quality, which are the Mutual Information (MI), entropy, and Standard Deviation (St. Dev.). The MI shows that the fused image might have valuable information of both original images. The entropy shows that the fused image carries average information. The St. Dev. shows the statistical distribution of fused image. In the first simulation, we use

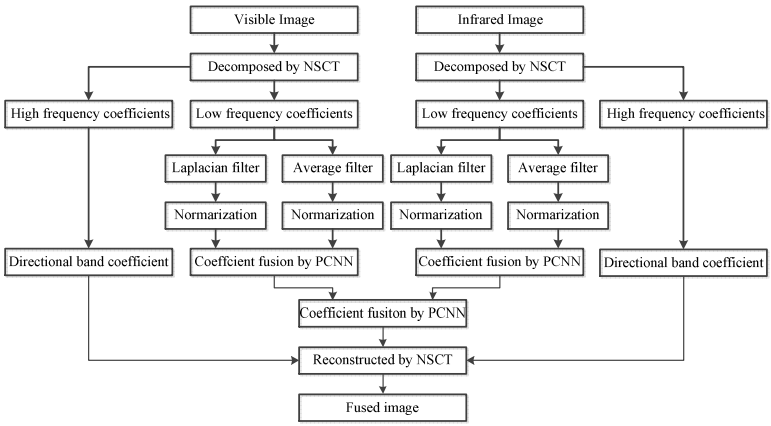

Figure 3: The proposed image fusion algorithm.

the original images in Fig. 4, and the fused images are shown in the Fig. 5. From the Fig. 5, we can see that the original images are fused well and its visual performance is as good as original images. .

(a) Visible image. (b) Infrared image.

Figure 4: Target images for image fusion.

(a) PCNN with NSCT. (b) Proposed algorithm.

Figure 5: Fused image by different methods.

Table 1 shows the experimental results and comparisons for the image fusion performance in the Fig. 4. From this results we can see that the proposed image fusion algorithm has better quality of fused image than the PCNN. It means that the original images held the characteristics even if the original images are processed by two filters, namely laplacian and average filters. We focus on the low frequency coefficients for the localized property and edge enhancements of the original coefficients by using the both filters, hence the mutual information, entropy and standard deviation are much improved, respectively. Especially, the proposed method has a high MI performance and a high standard deviation of the fused image. In the proposed model, the coefficients are preprocessed by the filters, thereby the original image is varied. However, the result of the proposed method obtains the high MI performance. The standard deviation generally shows the edge performance. The PCNN responds the edge. The proposed method enhances the edge by the laplacian filter from the original image coefficients. In the conventional method, the fused image is made from original images. Thus, the fused image has only characteristics of the original image.

Table 1: Fusion performance index of different methods.

	MI	Entropy	St. Dev.
PCNN+NSCT	2.4956	7.0300	32.713
Proposed	2.8358	7.1275	34.865

In the next simulation, we use the test images and can obtain the fused images as shown in Fig. 6 and Fig. 7 respectively. From the Fig. 7, we can see that the original images are fused well and its visual performance is as good as original images.

From Table 2, the proposed image fusion algorithm has better quality of fused image than the image fusion of the PCNN. The mutual information and the standard deviation are improved well. This result's trend is similar to the Table. 1. Thereby, we can say that the proposed method has a better image fusion performance than the conventional method.

Table 2: Fusion performance index of different .

	MI	Entropy	St. Dev.
PCNN+NSCT	5.5801	7.4862	53.454
Proposed	6.0821	7.5491	54.669

(a) Visible image. (b) Infrared image.

Figure 6: Target images for image fusion.

(a) PCNN with NSCT. (b) Proposed algorithm.

Figure 7: Fused image by different methods.

5 CONCLUSIONS

In this paper, we have proposed the novel image fusion algorithm for visible and images by using NSCT and PCNN. We processed the low frequency coefficients which are decomposed by the NSCT, in addition filtered by the laplacian and the average filter. There, the coefficients were fused by the PCNN. Finally, the fused image is reconstructed using the low frequency and high frequency coefficient by the inverse NSCT. From experimental results, the proposed image fusion algorithm has better quality than the image fusion performance for using the PCNN only.

REFERENCES

da Cunha, A., Zhou, J., and Do, M. (2006). The nonsubsampled contourlet transform: Theory, design, and applications. *IEEE Transaction on Image Processing*, 15(10):3089–3101.

Eckhorn, R. (1990). Feature linking via synchronization among distributed assemblies: Simulations of result from cat visual cortex. *Neural Computation*, 2:293–307.

Ge, Y. and Li, X. (2010). Image fusion algorithm based on pulse coupled neural networks and nonsubsampled contourlet transform. *Proc. Second International Workshop on Education Technology and Computer Science*, 3:27–30.

Jhonson, J. and Padgett, M. (1999). Pcnn models and applications. *IEEE Transactions of Neural Network*, 10(3):480–498.

Lindblad, T. and Kinser, J. (2005). *Image Processing using Pulse-Coupled Neural Networks*. Springer Publisher.

Liu, F., Li, J., and Huang, C. (2012). Image fusion algorithm based on simplified pcnn in nonsubsampled contourlet transform domain. *International Workshop on Information and Electronics Engineering*, 29:1434–1438.

Qu, X., Yan, J., Xiao, H., and Zhu, Z. (2008). Image fusion algorithm based on spatial frequency-motivated pulse coupled neural networks in nonsubsampled contourlet transform domain. *Acta Automatica Sinica*, 34(12):1508–1514.

Wang, M., Peng, D., and Yang, S. (2008). Fusion of multiband sar images based on nonsubsampled contourlet and pcnn. *Proc. 4th International Conference on Natural Computation*, pages 529–533.

Xu, B. and Chen, Z. (2004). A multisensor image fusion algorithm based on pcnn. *Proc. the 5th World Congress on Intelligent Control and Automation*, pages 3679–3682.

Yang, G., Wetering, H. V. D., Hou, M., Ikuta, C., and Liu, Y. (2010). A novel design approach for contourlet filter banks. *IEICE Transactions on Information and Systems*, E93-D(7):2009–2011.

Yang, S., M. Wang, Y. L., Qi, W., and Jiao, L. (2009). Fusion of multiparametric sar images based on sw-nonsubsampled contourlet and pcnn. *Signal Processing*, 89(12):2596–2608.

Zhou, J., da Cunha, A., and Do, M. (2005). Nonsubsampled contourlet transform: Construction and application in enhancement. *Proc. International Conference on Image Processing*, pages 469–472.